Mach stem formation in outdoor measurements of acoustic shocks

Kevin M. Leete,[a] **Kent L. Gee, and Tracianne B. Neilsen**
Department of Physics and Astronomy, Brigham Young University, Provo, Utah 84602, USA
kevinmatthewleete@gmail.com, kentgee@byu.edu, tbn@byu.edu

Tadd T. Truscott
Department of Mechanical and Aerospace Engineering, Utah State University, Logan, Utah 84322, USA
taddtruscott@gmail.com

Abstract: Mach stem formation during outdoor acoustic shock propagation is investigated using spherical oxyacetylene balloons exploded above pavement. The location of the transition point from regular to irregular reflection and the path of the triple point are experimentally resolved using microphone arrays and a high-speed camera. The transition point falls between recent analytical work for weak irregular reflections and an empirical relationship derived from large explosions.

Date Received: August 21, 2015 **Date Accepted:** December 1, 2015

1. Introduction

This Letter describes the irregular reflection and Mach stem formation of acoustic shock waves generated by explosions. From Mach's original investigation,[1] regular reflection of a shock wave consists of the incident and reflected shocks that intersect at the reflecting surface, whereas irregular reflections consists of three shocks: the incident shock, a reflected shock, and a Mach stem that travels parallel to the surface. The height of intersection of the three shocks, referred to as the triple point, grows with propagation distance. Subsequent studies by von Neumann[2] and others for steady shocks resulted in a theoretical paradox,[3] where irregular reflections were observed in theoretically disallowed regimes, primarily with shock Mach numbers less than $M_s = v_s/c_0 = 1.47$[4], where v_s is the velocity of the shock wave and c_0 is the ambient sound speed. Recent investigations have shown that actual reflections are not as simple as the presence of two or three straight shocks,[4–6] resulting in various classifications. According to Semenov *et al.*,[7] two types of irregular reflection that could occur in this regime are von Neumann reflection and Mach reflection. Although von Neumann reflections and Mach reflections both form a Mach stem, the interaction of weaker waves in the case of the von Neumann reflection results in a continuous slope between the Mach stem and incident shock wave at the triple point. Mach reflections, on the other hand, have a slope discontinuity between the incident shock and Mach stem at the triple point and a slipstream that trails behind the triple point trajectory.

The irregular reflection of spherical unsteady shocks, such as those generated by an explosion above a flat surface, is more complex because the amplitude of the shock and the angle of incidence, φ, both decrease with propagation distance; the former discourages irregular reflection, while the latter encourages it. Generally for the case of an explosion over a rigid surface, regular reflection occurs close to the source, and as the shock propagates outward it transitions to irregular reflection. Although there are no analytical solutions for the transition from regular to irregular reflection, various approaches have been employed. First, the shock has been treated as steady at each propagation point to determine whether a regular or irregular reflection could occur.[3] The validity of this method is in question because of observed hysteresis effects.[8] Second, Baskar *et al.*[9] recently introduced a critical parameter derived from the nonlinear Khokhlov-Zabolotskaya-Kuznetsov equations to describe the transition of an unsteady shock from regular to different types of irregular reflection: $a \approx 0.85 \sin\varphi/\sqrt{M_a}$ in air, where $M_a = \Delta P/\gamma P_0$ is the peak acoustic Mach number calculated from the pressure change across the shock, ΔP, γ is the ratio of specific heats, φ is the angle relative to the ground plane, and P_0 is the ambient pressure. However, Karzova *et al.*[10] experimentally

[a]Author to whom correspondence should be addressed.

found that for weak shocks generated by spark pulses the transition point did not compare with those predicted by a for all cases. Finally, empirical fits[11,12] to data from large explosions allow the calculation of Mach stem formation distance, triple point height, and stem overpressure as functions of the distance of the explosion from the reflecting surface (otherwise known as the height-of-burst, or HOB) and equivalent yield in kilotons of TNT (kt TNT). However, given the disparities in scales and type of explosion, the validity of applying these fits to small-scale gaseous explosions approaching the acoustical weak-shock regime is in question.

In this Letter, we describe a regime that has not been previously documented: acoustical and visual observations of irregular reflections of acoustic shocks generated from gaseous explosions whose peak acoustic Mach numbers range from $0.02 < M_a < 0.5$ and shock Mach numbers from $1.01 < M_s < 1.3$ at the points of reflection across the angular range $6° < \varphi < 48°$. Comparisons are made against both the equivalent HOB empirical fits based on high explosives and the parameter, a, which was derived for lower-amplitude shocks. The transition from regular to irregular reflection for the spherical, unsteady shocks generated by the explosions is found to occur between the scaled empirical relation and the a-based estimates.

2. Experiment description

Recent related studies have shown that spherical oxyacetylene balloons are reliable sources of weak shock waves[13] and identified the presence of irregular reflections in outdoor measurements.[14] The current experiment, shown in Fig. 1, is similar to the one conducted in Ref. 14. The x axis is defined as the horizontal range along the propagation line from the point directly below the balloon, and the z axis is the height above the pavement. The 0.685 m diameter balloons, filled with a stoichiometric mix of acetylene and oxygen, were placed in a tripod-mounted metal cradle, with the balloon center at $z = 1.8$ m. Two PCB pressure probes (models 112A23 and 137B24B) were located on tripods at fixed distances (1.35 and 1.27 m) at about 45° on either side of the x axis at HOB to be used as references. Over the 25 detonations, the mean peak sound pressure levels were 194.2 and 195.6 dB re 20 μPa with standard deviations of 0.35 and 0.50 dB, respectively. The waveforms in this experiment are similar in shape to those shown in Ref. 14 for propagation distances of less than 10 m. A tripod with an array of GRAS 6.35 mm, 46BG pressure microphones attached at $z = 0.03$, 0.05, 0.10, 0.20, 0.30, 0.91, and 1.83 m was placed at 15 different locations in x throughout the test to scan the length of the propagation line. An additional PCB 112A23 probe was attached to the end of a tripod with an adjustable boom arm to provide additional resolution at areas of interest. To minimize scattering, all probes and microphones were taped to the end of 9.5 mm diameter wooden dowels which extended horizontally from the tripods. Pressure waveforms were recorded using a system comprised of National Instruments PXI-4462 dynamic signal acquisition devices with a sampling frequency of 204.8 kHz. A Kestrel 4500BT weather meter was used to log the ambient temperatures, pressures, humidity, and wind speed and direction for each test. The ambient pressure used in calculating M_a was relatively constant at 87 kPa during the experiments and the wind was low enough to be considered negligible.

To visualize the shockwave propagation, a Phantom v1610 high-speed camera operating at 18 002 frames per second recorded 4 separate regions along the propagation line: $x = 3.35$ to 5.79 m, 2.13 to 4.57 m, 6.10 to 8.53 m, and 9.14 to 11.58 m. In

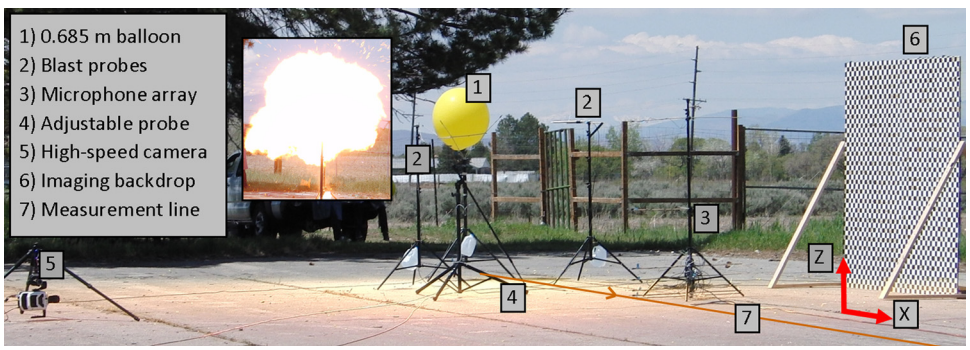

Fig. 1. (Color online) Mach-stem experiment setup with (1) gas-filled balloon in its metal cradle at z = 1.8 m; (2) two reference pressure gauges at 1.35 and 1.27 m; (3) vertical array of GRAS pressure microphones; (4) pressure probe attached to adjustable boom arm; (5) phantom high-speed camera; (6) high-contrast checkerboard backdrop; and (7) line of propagation (x axis). (Inset) Balloon explosion.

these regions, a 2.4×2.4 m checkerboard backdrop was placed 3.05 m behind the propagation line to provide additional contrast for the camera. The checkerboard squares were fairly large at 4.8 cm on a side, which was chosen for ease of construction. Though the checkerboard was an improvement over the ambient background, especially where the shock crossed over the border between the black and white squares, a smaller checkerboard pattern would have aided in the visualization of the shock. To calibrate the recorded video to physical locations in space for each setup, the backdrop was moved up to the x axis and a still photo was taken. In post processing, the position of the shock is emphasized by subtracting the pixel values of two adjacent frames of the video. These difference images were then converted to gray scale and their histograms readjusted so that all pixels above a certain threshold value were saturated to white and all remaining pixel values were linearly distributed from black to white. A median filter in a 5×5 pixel neighborhood was then applied to reduce noise. Finally, to increase visibility of the shock, a color map varying from deep red to white was used. A clearer visualization would have been achieved if a Schlieren type setup was used, though it would have been complicated to implement in the outdoor setting of this experiment.

3. Results

3.1 Triple point and transition point localization

Displayed in Mm. 1 is a compilation of the processed high speed video from the four regions along the propagation line as well as an explanatory introduction. Microphone positions as well as a cubic fit to estimated triple point positions (as taken from Fig. 3) are overlaid on the video. The incident shock can be seen coming in from the left and propagating across the screen with the reflected shock close behind. As the shocks propagate, it is seen that they merge, creating the characteristic "Y" pattern of a Mach stem. The triple point is relatively easy to identify in most of the video, with two exceptions. First, because the camera was hung a short distance above the ground and the backdrop was offset from the propagation line, between $0 \leq z \leq 5$ cm the image background is the concrete, with insufficient contrast to extract exact position values for the triple point. Second, beyond $x = 9.14$ m, the shock strength had decreased sufficiently that even with the image processing, estimation of the triple point via visual methods is less trustworthy. In both of these regions, the visual imagery is regarded as supporting evidence for the acoustic data. Additional shock-like shadows can be seen both ahead of, and behind, the explosion-generated Mach stem, and seem to be propagating along the backdrop or along the ground. Whether these are artifacts of the camera focusing, image processing, or physical surface waves has not been determined.

Mm. 1. Compiled high-speed video from the four setup positions with explanatory introduction and selected data from Fig. 3 overlaid. This is file type mpeg (40.2 Mb)

The spatial sampling of the acoustic data gives a more accurate representation of the position of the triple point, based on examining the waveform for the presence of one or two shocks. Identification of two shocks in a given waveform indicates that the incident and reflected waves both reached the microphone at that location, meaning that either a regular reflection occurred or the triple point passed below the microphone. Conversely, a single shock in the waveform signifies that the Mach stem was at least as tall as the microphone height. An illustrative example is given in Fig. 2. Figures 2(a) and 2(c) show a single frame of the high-speed video with the locations of three 46BG microphones superimposed at $x = 4.6$ and 6.9 m, respectively. Figures 2(b) and 2(d) show pressure waveform segments for the three microphones at the same locations. As seen in Fig. 2(b), at $z = 0.10$ m a single shock is present in the acoustic data, corroborated by the Mach stem passing through the image of Fig. 2(a). Further, the incident and reflected shocks are both present at $z = 0.20$ and $z = 0.30$ m, which is verified by the two unmerged shocks of Fig. 2(a). Consequently, the position of the triple point can be identified between $z = 0.10$ and 0.20 m. Figures 2(c) and 2(d) show similar data, but at $x = 6.9$ m. At this distance, the image in Fig. 2(c) has more uncertainty in the triple point position due to the lower signal strength. However, the acoustic data shown from two closely spaced microphones allow for the identification of the triple point location between $z = 0.36$ and 0.38 m.

Because the shock amplitudes were consistent between explosions at the reference microphones, the data can be compiled to yield one cross-section of the growth of the triple point along the x - z plane, as shown in Fig. 3. The blue triangles correspond to microphones that recorded a single shock (Mach stem) while the red triangles correspond to double shock events (incident and reflected). The green dots correspond to

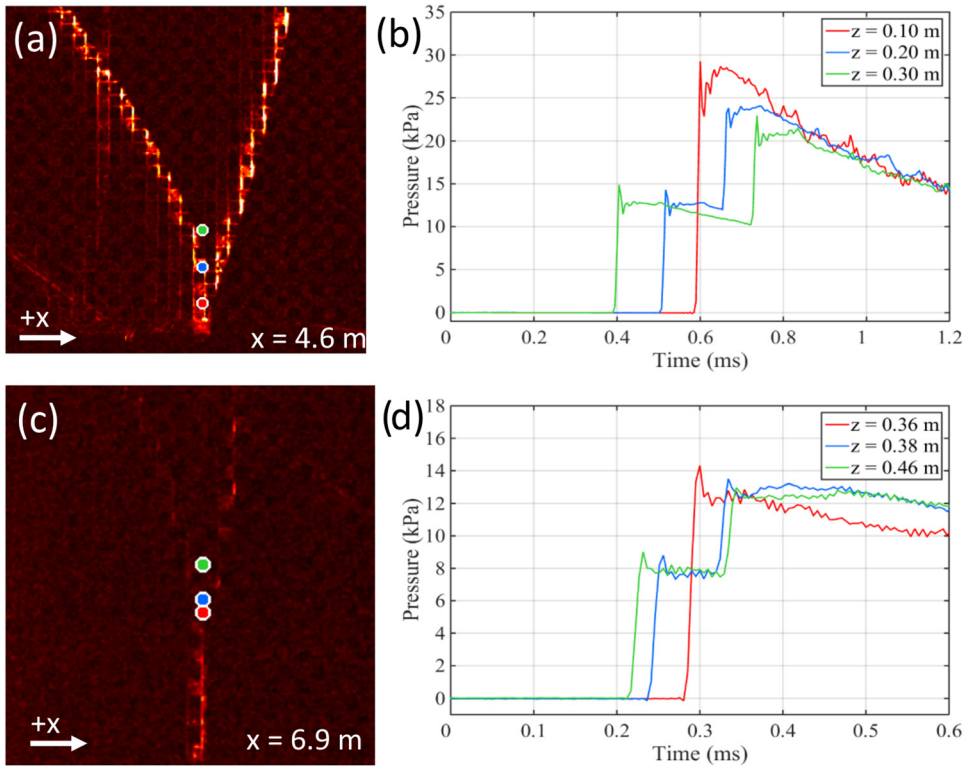

Fig. 2. (Color online) Two methods for identifying triple point location: (1) A single frame of high-speed video (a) showing the irregular reflection of a shock wave at $x = 4.6$ m downstream from the source. (2) A pressure vs time graph (b) of three separate microphones located at different heights at $x = 4.6$ m with relevant positions superimposed as the colored dots on (a). (c) and (d) are similar images and pressure measurements at $x = 6.9$ m.

estimates of the triple point position as taken from the high-speed video. A cubic polynomial, represented by the dashed black line, was fitted to several points where the vertical resolution of the triple point was within 2.54 cm. These points ($x = 2.74$, 3.05, 3.66, 6.10, 6.86 11.05, and 16.38 m) are displayed with yellow dots. A cubic fit was chosen in accordance with previous works.[11] The location of the $z = 0$ crossing is determined to be the transition point from regular to irregular reflection, x_0: for this experiment, $x_0 = 2.56\,\text{m} \pm 0.1\,\text{m}$.

3.2 Comparison of transition point to predictions

The empirical equations from Needham require that we scale our experiment to the equivalent problem of a 1 kt of TNT blast at a certain HOB.[11] Multiplying the heat of combustion of acetylene[15] by the number of moles of acetylene in the balloon gives an

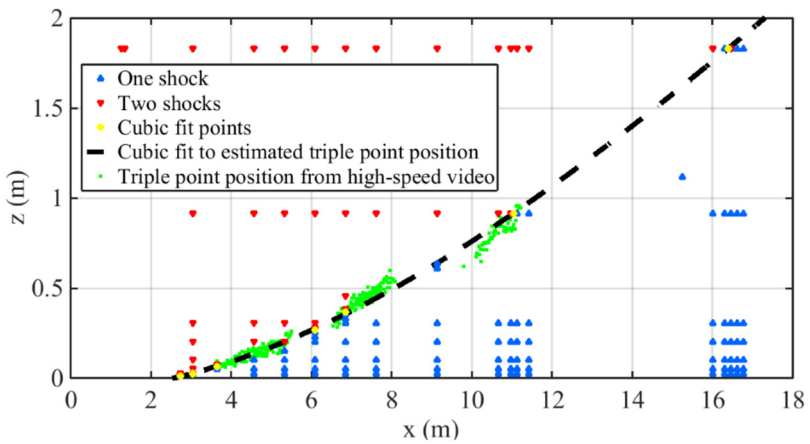

Fig. 3. (Color online) Identification of triple point location for the oxyacetylene explosions, with the red and blue triangles used to identify whether a Mach stem was observed. Green dots represent the position of the triple point extracted from the high-speed footage. The black dashed line is a cubic fit to several points (yellow dots) from the acoustic data where the vertical resolution of the triple point position was within 2.54 cm.

estimation of the energy released by the explosion. Appropriately scaling the distances by using the equivalent yield of 5.26×10^{-7} kt of TNT, the configuration in this experiment corresponds to the equivalent problem of 1 kt TNT exploded with HOB = 227 m. Equation (1) corrects[16] an empirical equation given by Needham[11] in cgs units for the horizontal range at which the transition from regular to irregular reflection occurs for a 1 kt TNT explosion in terms of HOB

$$x_N = \left(\frac{170\,\mathrm{HOB}}{1 + 25.05\,\mathrm{HOB}^{0.25}}\right) + (1.7176 \times 10^{-7})\mathrm{HOB}^{2.5}. \quad (1)$$

Substitution of the scaled HOB results in $x_N = 2.08 \pm 0.02$ m for our experiment.

To analytically solve for the point of transition from irregular to regular reflection, the peak acoustic pressure for the incident shock wave was plotted as a function of radial distance from the center of the balloon. This was least-squares fit to a curve, then using the geometry of the setup the corresponding radial distances were mapped to specific x-values along the propagation line with corresponding values of φ. The acoustic Mach number and the parameter a were subsequently calculated. The derivation in Baskar *et al.*[9] predicts that the transition from regular to irregular reflection occurs at $a = 0.8$. However, in Karzova *et al.*,[10] which involved weaker shocks than those here, the transition point was experimentally observed to take place at $a = 1.1 \pm 0.3$ for $M_a = 0.006$ and $a = 1.05 \pm 0.15$ for $M_a = 0.044$.

In our experiment, as the shock propagates, the Mach number and the angle of incidence vary and the corresponding values of the critical parameter change from $a = 0.9$ at $x = 0$ to $a = 0.46$ at $x = 18$ m. Based on the measurement geometry and acoustic data, the transition criterion of $a = 0.8$ corresponds to a horizontal range of $x_B = 2.88 \pm 0.3$ m. The estimated uncertainty stems from applying the peak level variation at the reference probes to the calculation of M_a. It should be noted that the observed mean value of the transition criterion in Karzova *et al.* is greater than the range of a values obtained in our experiment, implying that irregular reflection should be present at the ground directly under the explosion, at $x_K = 0$ m. This is not the case. However, within the noted uncertainty for $M_a = 0.006$, the Mach stem formation distance could occur anywhere from $x_K = 0$ to $x_K = 2.88 \pm 0.3$ m, which spans the observed transition range of $x_0 = 2.56 \pm 0.1$.

The observed transition point, x_0, is similar, but falls between, the locations predicted for lower amplitude sources and the empirical formulas from large explosive yields. The Baskar *et al.* analytical value $a = 0.8$ overestimates x_0, while x_N derived from large scale explosions underestimates it. The details of the derivation of the critical parameter provide a clue as to a possible explanation for the overestimation. In Baskar *et al.*, the criterion for a was derived for the transition from regular to von Neumann reflection. However, the reflections observed in this experiment appear to have a slope discontinuity in the shock front, which characterizes a single Mach reflection. This is faintly seen in pane 2 of the high speed video where there is a slope discontinuity at the connection of the incident wave and the Mach stem. Concrete identification of the type of irregular reflection present in this experiment would require a clearer picture of the slope discontinuity as well as require the visualization of a slipstream trailing from the triple point. Evidence of a slipstream is absent in the high-speed video, although it is improbable that the imaging techniques used were sensitive enough to record it.

4. Concluding discussion

We have observed, through both acoustic data and high-speed video imaging, the transition from regular to irregular reflection of shock waves and Mach stem growth in a regime not previously studied. Although the high-speed video effort was limited by the preliminary nature of our experiment, it provides sufficient evidence to verify the acoustical methods used to localize the triple point position. A previous empirical estimate,[11] derived from explosions several orders of magnitudes greater, underestimate the observed transition point. Conversely, estimates based on an analytical solution,[9] derived for weaker shocks in a regime for von Neumann reflections, overestimates the transition point. Thus, the experimental observations point to the need for additional theoretical work to model these types of irregular reflections.

Acknowledgments

The authors are grateful to the BYU Office of Research and Creative Activities for Undergraduate Research and Mentoring Environment Grants. Dr. Gabi Ben-dor, Dr. Charles Needham, Dr. David Blackstock, and Dr. Maria Karzova are also gratefully

acknowledged for their helpful communications. In addition, Dr. Jeffrey Macedone provided safety training on filling the acetylene-oxygen balloons and input on the combustion. Finally, Jonathon Pendlebury assisted with a preliminary version of the experiment analyzed here.

References and links

[1]E. Mach, "Uber den Verlauf Von Funkenwellen in der Ebene und im Raume," Sitzungsbr. Akad. Wiss. Wein **78**, 819–838 (1878).

[2]J. von Neumann, "Oblique reflection of shocks," in *John von Neumann Collected Works*, edited by A. H. Taub (MacMillan, New York, 1963), Vol. 6, pp. 238–299.

[3]G. Ben-Dor, *Shock Wave Reflection Phenomena* (Springer Verlag, New York, 2007), pp. 3–4 and 297–303.

[4]P. Colella and L. F. Henderson, "The von Neumann paradox for the diffraction of weak shock waves," J. Fluid Mech. **213**, 71–94 (1990).

[5]E. I. Vasiliev and A. N. Kraiko, "Numerical simulation of weak shock diffraction over a wedge under the von Neumann paradox conditions," Comput. Math. Phys. **39**, 1335–1345 (1999).

[6]B. Skews and J. Ashworth, "The physical nature of weak shock wave reflection," J. Fluid Mech. **542**, 105–114 (2005).

[7]A. N. Semenov, M. K. Berezkina, and I. V. Krassovskaya, "Classification of pseudo-steady shock wave reflection types," Shock Waves **22**, 307–316 (2012). For simplicity, the "Single Mach-Smith Reflections" as described in this reference are referred to as "Mach reflections" in this Letter.

[8]M. Geva, O. Ram, and O. Sardot, "The non-stationary hysteresis phenomenon in shock wave reflections," J. Fluid Mech. **732**, R1–R11 (2013).

[9]S. Baskar, F. Coulouvrat, and R. Marchiano, "Nonlinear reflection of grazing acoustic shock waves: Unsteady transition from von Neumann to Mach to Snell-Descartes reflections," J. Fluid Mech. **575**, 27–55 (2007).

[10]M. M. Karzova, V. A. Khokhlova, E. Salze, S. Ollivier, and P. Blanc-Benon, "Mach stem formation in reflection and focusing of weak shock acoustic pulses," J. Acoust. Soc. Am. **137**, EL436–EL442 (2015).

[11]C. E. Needham, *Blast Waves* (Springer, New York, 2010), pp. 216–217.

[12]ANSI S2.20-1983: *American National Standard for Estimating Airblast Characteristics for Single Point Explosions in Air* (Acoustical Society of America, New York, 2006).

[13]M. B. Muhlestein, K. L. Gee, and J. H. Macedone, "Educational demonstration of a spherically propagating acoustic shock," J. Acoust. Soc. Am. **131**, 2422–2430 (2012).

[14]S. M. Young, K. L. Gee, T. B. Neilsen, and K. M. Leete, "Outdoor measurements of spherical acoustic shock decay," J. Acoust. Soc. Am. **138**, EL305–EL310 (2015).

[15]R. A. Kafiatullin, S. A. Eremin, and E. V. Sagadeev, "Calculation of heats of combustion of acetylene hydrocarbons," Theoretical Found. Chem. Eng. **41**, 221–224 (2007).

[16]Equation (1) was incorrectly typeset in Ref. 11; private correspondence with Dr. Needham gave the revised equation used here. For the purposes of this Letter the name of the variable was changed from R_0 to x_N.